There is no significant difference in intermolecular hydrogen bonding between *m*-Cl-DPP and *p*-Cl-DPP as seen in the previous section. A striking difference is, however, found in the π–π overlap along the stacking axis of the molecules (Figs. 5*a* and 5*b*). The overlap is quite insignificant in *p*-Cl-DPP, so that the basic molecular absorption characteristics remain almost unchanged even in the solid state. By contrast, the molecular nature of *m*-Cl-DPP is appreciably perturbed by strong π–π interactions in the solid state so as to give a different optical absorption spectrum.

Further details on this subject are given in our previous report (Mizuguchi & Rihs, 1992).

The authors would like to express their sincere thanks to Messrs E. Baeriswyl, G. Giller, H. Walliser and H. R. Walter for experimental assistance.

References

B. A. Frenz & Associates Inc. (1985). *Enraf–Nonius SDP-Structure Determination Package*. Version 1.1. College Station, Texas, USA.

Charbonneau, G.-P. & Delugeard, Y. (1976). *Acta Cryst.* B**32**, 1420–1423.

Iqbal, A., Cassar, L., Rochat, A. C., Pfenninger, J. & Wallquist, O. (1988). *J. Coat. Tech.* **60**, 37–45.

Johnson, C. K. (1971). *ORTEP*. Report ORNL-3794. Oak Ridge National Laboratory, Tennessee, USA.

Main, P., Fiske, S. J., Hull, S. E., Lessinger, L., Germain, G., Declercq, J.-P. & Woolfson, M. M. (1978). *MULTAN*11/78. *A System of Computer Programs for the Automatic Solution of Crystal Structures from X-ray Diffraction Data*. Univs. of York, England, and Louvain, Belgium.

Main, P., Fiske, S. J., Hull, S. E., Lessinger, L., Germain, G., Declercq, J.-P. & Woolfson, M. M. (1982). *MULTAN*11/82. *A System of Computer Programs for the Automatic Solution of Crystal Structures from X-ray Diffraction Data*. Univs. of York, England, and Louvain, Belgium.

Mizuguchi, J. (1981). *Krist. Tech.* **16**, 695–700.

Mizuguchi, J., Grubenmann, A., Wooden, G. & Rihs, G. (1992). *Acta Cryst.* B**48**, 696–700.

Mizuguchi, J. & Rihs, G. (1992). *Ber. Bunsenges. Phys. Chem.* **96**, 597–606.

Mizuguchi, J. & Wooden, G. (1991). *Ber. Bunsenges. Phys. Chem.* **95**, 1264–1274.

Pauling, L. (1960). *The Nature of the Chemical Bond and the Structure of Molecules and Crystals*. Ithaca: Cornell Univ. Press.

Rochat, A. C., Cassar, L. & Iqbal, A. (1986). US Patent 4 579 949.

Acta Cryst. (1993). B**49**, 1060–1068

Structure of the Incommensurate Phase of 4,4′-Dichlorobiphenyl Sulfone at 90 K

By F. J. Zúñiga, J. M. Pérez-Mato and T. Breczewski

Departamento de Fisica de la Materia Condensada, Facultad de Ciencias, Universidad del Pais Vasco, Apdo. 644, Bilbao, Spain

(*Received* 5 *March* 1993; *accepted* 3 *August* 1993)

Abstract

The structure of the incommensurate phase of 4,4′-dichlorobiphenyl sulfone, $(ClC_6H_4)_2SO_2$, has been determined at 90 K using the superspace formalism. Refinement of the atomic modulation, which is of a displacive type, with wavevector $\mathbf{q} = 0.780\ (2)\mathbf{b}^*$, has been performed in the superspace group $P(I2/a)$: $(s,-1)$, using main and first-order satellite reflections. A model of the distortion including zero, first- and second-order harmonics has been considered in the modulation. The final agreement factors are $R = 0.042$, $R_0 = 0.039$ and $R_1 = 0.044$ for all, main and first-order satellite reflections, respectively. Second-order harmonics are critical in the refinement as they decrease the R_1 factor from 0.12 down to 0.043. The primary distortion corresponds to a displacive mode of A_2 symmetry, with atomic displacements reaching up to 0.3 Å. It involves intermolecular librational and translational motions and a significant intramolecular twist of the phenyl groups. The secondary distortion given by the second harmonic in the modulation has a much smaller amplitude and includes a slight bending of the molecule. Crystal data of the average structure: $T = 90$ K, $M_r = 287.2$, monoclinic, $I2/a$, $a = 20.20\ (2)$, $b = 4.910\ (2)$, $c = 12.054\ (9)$ Å, $\beta = 90.02\ (4)$, $V = 1195\ (2)$ Å^3, $Z = 4$, $D_x = 1.597$ Mg m^{-3}, λ(Mo $K\alpha$) = 0.7107 Å, $\mu = 0.67$ mm^{-1}, $F(000) = 584$.

1. Introduction

The compound 4,4′-dichlorobiphenyl sulfone, $(ClC_6H_4)_2SO_2$ (hereafter DCBPS), is currently attracting great interest due to the stability of an incommensurate phase at low temperature. Pusiol, Wolfenson & Brunetti (1989), on the basis of ^{35}Cl NQR measurements, proposed for the first time the incommensurate nature of this phase, which is stable

ISSN 0108-7681 ©1993

below 150 K. These authors also refer to the existence of a lock-in transition at 115 K. Since the publication of that work, other studies on DCBPS have confirmed the phase transition (normal–incommensurate) at 150 K, but some controversy remains about the existence of the lock-in transition.

At room temperature crystals of DCBPS are monoclinic (normal phase), $I2/a$, $a = 20.216$, $b = 5.004$, $c = 12.148$ Å, $\beta = 90.57°$ (Sime & Woodhouse, 1974). The incommensurate phase was confirmed and the modulation characterized by means of X-ray diffraction measurements by Kasano, Koshiba, Kasatani & Terauchi (1990), who found the incommensurate modulation to be one-dimensional with a modulation wavevector $\mathbf{q} = \mathbf{a}^* + (\frac{1}{5} + \delta)\mathbf{b}^*$, δ varying between 0.021 and 0.014 in the temperature range 150–20 K, and with no lock-in transition detected in this temperature interval.

The results of AC calorimetry (Saito, Kamio, Kikuchi & Ikemoto, 1990) and adiabatic calorimetry (Tanaka, Saito, Nakayama, Eguchi & Atake, 1991) experiments confirmed the transition at 150 K and detected an anomaly at 115 K. More recent NQR measurements also found additional anomalies at 123 and 115 K (Nakayama, Eguchi & Kishita, 1992). On the other hand, Raman spectroscopy and birefringence studies (Ishii, Nakayama, Sakato & Kano, 1992) detected the transition at 150 K, but no anomaly corresponding to an additional transition at lower temperature was found.

More recently, elastic neutron measurements (Etrillard, Even *et al.*, 1993), ^{35}Cl NQR and calorimetric measurements (Etrillard, Toudic *et al.*, 1993) have indicated that the incommensurate phase is stable down to the lowest temperature investigated (4.5 K). The temperature behaviour of satellite reflections reveals the presence of high-order satellite reflections (up to fourth order at 13 K), with intensities increasing on cooling. These results have been interpreted as being due to the evolution from a sinusoidal structural modulation, in the high-temperature region, towards a strong anharmonic modulation at lower temperatures, always in the same incommensurate phase.

The microscopic mechanism driving the incommensurate structural instability in DCBPS is particularly interesting due to the possible similarity to the extensively studied compound biphenyl ($C_{12}H_{10}$) (Cailleau, 1986). Raman measurements (Ishii, Nakayama, Sakato & Kano, 1992) indicate that a soft-mode also exists in DCBPS. Despite differences in the sequence of transitions in the two compounds, it is to be expected that, as in the case of biphenyl, competition between intramolecular and intermolecular forces is responsible for the transition. In the case of DCBPS, this mechanism has been analyzed by studying the lattice dynamics of the compound using empirical models (Saito, Kikuchi & Ikemoto, 1992). Within a rigid-body approximation for DCBPS molecules, the lowest calculated phonon branch shows a softening at about $0.8\mathbf{b}^*$, in agreement with the modulation wavevector in the incommensurate phase (see next section). The minimum in the phonon branch at about $0.8\mathbf{b}^*$ becomes much sharper if twisting of the phenyl rings within the DCBPS molecule is allowed. Both lattice dynamics simulations and Raman measurements seem to indicate that the soft-mode includes a significant intramolecular twisting of the phenyl rings in the molecule (Ishii, Nakayama, Sakato & Kano, 1992). However, a complete understanding of the nature of the incommensurate structural instability in this compound is still lacking.

In this paper, the structure of the incommensurate phase of DCBPS at 90 K is determined using the superspace-group formalism and the modulation obtained is analyzed in terms of frozen intermolecular and intramolecular symmetry modes.

2. Experimental

Colourless crystals of DCBPS were obtained by slow evaporation of an ethanol solution of high-quality compound (commercially available). Precession photographs of $(h,k,0)$, $(h,k,1)$, $(0,k,l)$ and $(1,k,l)$ layers were taken at 100 K using an open-flow gas cryostat (Cosier & Glazer, 1986). These photographs clearly showed the set of main reflections defining the average lattice, a great number of first-order and a few second-order satellite reflections; the general symmetry observed was monoclinic. Systematic absences detected for the main reflections were compatible with the space group $I2/a$. All satellite reflections could be identified as first- ($m = 1$) or second- ($m = 2$) order satellites with the modulation wavevector $\mathbf{a}^* + 0.22\mathbf{b}^*$, as reported by Kasano, Koshiba, Kasatani & Terauchi (1990). However, a more convenient and simpler choice of modulation wavevector can be achieved by subtracting the lattice vector ($\mathbf{a}^* + \mathbf{b}^*$). Thus, all scattering vectors were indexed according to the expression:

$$\mathbf{H} = h\mathbf{a}^* + k\mathbf{b}^* + l\mathbf{c}^* + m\mathbf{q}$$

with the modulation wavevector $\mathbf{q} = 0.78\mathbf{b}^*$. Careful examination of the photographed layers showed the condition for the presence of satellite reflections:

$$(0,k,0,m) \quad k = \text{even and } m = \text{even}$$

which indicates the existence of a $\{C_{2y}|\ \frac{1}{2},0,0,\frac{1}{2}\}$ helical axis in the superspace group. At this point, the superspace group $P(I2/a)$:$(s,-1)$ (de Wolf, Janssen & Janner, 1981) was assumed. This symbol does not correspond to the standard one which requires transformation from an I-centred to a B-centred cell.

Table 1. *Summary of crystal data and data-collection parameters*

Crystal form	Prismatic
Crystal size (mm)	0.39 × 0.37 × 0.36
Temperature (K)	90
Reflections for lattice parameters	22 ($11 < \theta < 26°$)
Cell parameters (Å)	a = 20.20 (2)
	b = 4.910 (2)
	c = 12.054 (9)
	β = 90.02 (4)°
Modulation wavevector **q**	0.780 (3)**b***
$(\sin\theta/\lambda)_{max}$ (Å^{-1}) for ($hkl0$)	0.8071
$(\sin\theta/\lambda)_{max}$ (Å^{-1}) for ($hklm$)	0.7035
Check reflections	2 main, 1 satellite
$h,k,l,0$ limits	(±32, 7, 19)
h,k,l,m limits	(±26, 6, 16, ±1)
Scan width (°)	0.65 + 0.34tanθ
Scan speed (° min^{-1})	0.97–4.12
Measured reflections	6742
Independent reflections ($I > 3\sigma$)	6086 (5050)
Main	2625 (2192)
Satellite m = ±1	3456 (2855)
Satellite m = ±2	5 (3)
R_{int} without absorption corrections	0.0115
Main	0.008
Satellite	0.016
Weights	$1/\sigma^2(F)$
Max. shift/e.s.d.	0.01

However, in order to facilitate comparison with the room-temperature structure, the non-standard setting was used.

The temperature behaviour of the modulation wavevector was studied from the profiles of three satellite reflections measured at different temperatures from 145 down to 80 K. The results confirm a weakly temperature-dependent wavevector, in agreement with the results reported by Kasano, Koshiba, Kasatani & Terauchi (1990). A more accurate wavevector value $\mathbf{q} = 0.780\ (3)\mathbf{b}^*$ at 90 K was obtained from the profile of satellite reflections scanned along $\mathbf{b}^*$.

Crystal data and data-collection parameters are summarized in Table 1. Intensities were collected with a CAD-4 diffractometer equipped with the cryostat described above. Temperature stability was maintained within ±0.2 K during the measurement time. Collection of the main and associated first-order satellite reflections was carried out in sequential order, varying the index for satellites m first. Given the weakness and scarcity of second-order satellites observed on the photographs, no systematic collection of these reflections was attempted; only five of them, among the strongest ones, were included in the data set. Stability of the measurements and possible X-ray radiation damage to the structural modulation in the crystal was checked every 2 h by measuring the intensities of two main and one satellite reflections. At the end of the measurements, the intensity and shape of the check satellite reflections did not show significant changes. Data reduction and averaging of symmetry-equivalent reflections were carried out using a local version of the program system *XRAY*72 (Stewart, Kruger, Ammon, Dickinson & Hall, 1972) modified for one-dimensional modulated structures. Lorenz and polarization corrections were performed during refinement using the program *MSR* (Paciorek & Kucharczyk, 1985; Paciorek & Uszynski, 1987).

Table 2. *Representative elements of the superspace group P:($I2/a$):(s, −1) with wavevector* $\mathbf{q} = \delta\mathbf{b}^*$

$\{C_{2y}\mid \frac{1}{2},0,0,\frac{1}{2}\}$	$\{E\mid 1,0,0,0\}$
$\{I\mid 0,0,0,0\}$	$\{E\mid 0,1,0,-\delta\}$
$\{\sigma_y\mid \frac{1}{2},0,0,\frac{1}{2}\}$	$\{E\mid 0,0,1,0\}$
$\{E\mid \frac{1}{2},\frac{1}{2},\frac{1}{2},-\delta/2\}$	$\{E\mid 0,0,0,1\}$

3. Symmetry description and refinement

Representative elements of the proposed superspace group are given in Table 2. In the superspace formalism, each symmetry element can be described in the form $\{\mathbf{R}|\mathbf{t},\tau\}$, where $\mathbf{R}$ is a three-dimensional rotational operation, $\mathbf{t}$ is a fractional three-dimensional translation and τ a shift along the internal space (Janner & Janssen, 1980; Pérez-Mato, Madariaga, Zúñiga & Garcia-Arribas, 1987).

The modulated structure was assumed to be of a displacive type and possible modulation of the thermal parameters was neglected. Hence, in the refined structural model, only the atomic positions were considered modulated, so that the general expression for the position of an atom μ in a cell $\mathbf{l}$ is given by:

$$\mathbf{r}(\mathbf{l},\mu) = \mathbf{l} + \mathbf{r}_0(\mu) + \tfrac{1}{2}\sum_n \mathbf{u}_n(\mu)\exp\{2\pi i n\mathbf{q}.[\mathbf{l} + \mathbf{r}_0(\mu)]\} \quad (1)$$

where $\mathbf{r}_0(\mu)$ is the position of atom μ in the unit cell of what we can call an average structure; the sum excludes the term $n = 0$ and $\mathbf{u}_n(\mu)$ are complex vector amplitudes satisfying $\mathbf{u}_n(\mu) = \mathbf{u}^*_{-n}(\mu)$. The last term in (1) can be written more explicitly for each component as an atomic modulation function:

$$u_i(\mu,t) = \sum_{n>0} A_{n,i}(\mu)\cos\{2\pi[nt + \varphi_{n,i}(\mu)]\} \quad (i = x,y,z) \quad (2)$$

where $A_{n,i}$ and $\varphi_{n,i}(\mu)$ are the modulus and phase of the component $u_{ni}(\mu)$ of $\mathbf{u}_n(\mu)$; t is the internal coordinate, ranging from 0 to 1, which corresponds to the dense set of values $\mathbf{q}.[\mathbf{l} + \mathbf{r}_0(\mu)]$ in (1).

In the refinement with the *MSR* program, the structure was described in terms of the average coordinates $\mathbf{r}_0(\mu)$ and the amplitudes and phases given in (2), with the series only including first and second harmonics. In addition, as the sulfur atom S lies on a special position $(\frac{1}{4},y,0)$ of the average structure, its modulation parameters are symmetry restricted. In general, if $\{\mathbf{R}|\mathbf{t},\tau\}$ is a superspace symmetry operation and two atoms, μ and ν, are symmetry related by the operation $\{\mathbf{R}|\mathbf{t}\}$ in the average structure, the complex vector amplitudes, defined in (1), that

describe their atomic modulation functions are related by:

$$\mathbf{u}_n(\nu) = \mathbf{R}\mathbf{u}_{\Gamma(\mathbf{R})n}(\mu)\exp(-2\pi i n\tau_0) \qquad (3)$$

where $\Gamma(\mathbf{R}) = \pm 1$ if $\mathbf{Rq} = \pm\mathbf{q}$, and $\tau_0 = \tau + \mathbf{q}.\mathbf{t}$. Application of equation (3) to the S atom, invariant (in the average structure) for the operation $\{C_{2y}|\frac{1}{2},0,0\}$, yields the conditions:

$$u_{x,z,n}(\mathrm{S}) = (-1)^{n+1}u_{x,z,n}(\mathrm{S})$$
$$u_{y,n}(\mathrm{S}) = (-1)^n u_{y,n}(\mathrm{S}) \qquad (4)$$

which implies the restriction $u_{y,1}(\mathrm{S}) = 0$ for the first harmonic and $u_{x,z,2}(\mathrm{S}) = 0$ for the second.

Refinements were based on $|F|$ and performed in the full-matrix mode. Scattering factors for neutral atoms and anomalous-dispersion corrections were taken from *International Tables for X-ray Crystallography* (1974, Vol. IV).

Before refinement of the incommensurate structure, the average structure (without hydrogens) was refined with the *XRAY*72 system program using only the main reflections. Starting with the atomic positions of the room-temperature structure (Sime & Woodhouse, 1974), refinement with isotropic thermal displacements converged to an R value of 0.33. A few refinement cycles using anisotropic thermal parameters decreased the R factor to 0.087. As expected, in this refinement the atoms have anomalously large thermal displacements as they include the static modulation effect of the structure. In the next step, starting from the previous model with isotropic thermal parameters and taking into account only main reflections, the *MSR* program was used to refine the parameters of the average structure (without hydrogens) and the amplitudes of the first harmonics of the atomic modulations, with all the phases in (2), $\varphi_{n,\alpha}(\mu)$ $(n=1)$, fixed at zero. During this refinement the isotropic thermal displacements reduced considerably and, at the end, the refinement converged to $R = 0.10$. At this point, the satellite reflections were included in the observations with unit weights for all reflections [previously $w = 1/\sigma^2(F)$], and the phases $\varphi_{n,\alpha}(\mu)$ $(n=1)$ of the modulation functions were allowed to vary freely. The refinement converged slowly and in the final cycles thermal displacements were replaced by anisotropic ones (non-modulated), and weights changed to $1/\sigma^2(F)$. Finally, H atoms were included in the calculations and their atomic modulation functions refined; owing to the large correlation, only isotropic thermal displacements fixed to 0.011 Å^2 were considered for the hydrogens. Refinement of this model (with one harmonic only), showed rather high R factors: 0.088 for all reflections, with 0.060 for 2192 main reflections, and 0.122 for 2855 first-order satellite reflections. At this point, the refinement of a second-order harmonic for non-H atoms was attempted, first keeping all phases $\varphi_{n,\alpha}(\mu) = 0$ $(n=2)$, and then releasing all of the parameters. The introduction of the second harmonic in the refinement did not significantly change the amplitude or the phases of the first-order harmonic obtained from the previous refinement, but the R factors of all classes of reflections reduced to much lower values. The final agreement factors R (wR) were 0.042 (0.061) for all 5050 observed reflections, 0.039 (0.064) for 2192 main reflections, 0.044 (0.056) for 2855 first-order satellite reflections and 0.19 for three second-order satellite reflections; the global g.o.f. was 2.52 with 216 parameters varied in the refinement. The final atomic parameters including average coordinates, amplitudes and phases of the atomic modulations and equivalent isotropic thermal displacements are given in Table 3.* The interatomic distances and bond angles are listed in Tables 4 and 5.

Table 3. *Average coordinates and equivalent thermal displacements* (Å$^2 \times 10^2$) *of the incommensurate phase of DCBPS together with moduli (in relative units) and phases* ($/2\pi$) *of the displacive modulation functions*

For non-H atoms, first and second lines give first- and second-order harmonics respectively. Starred parameters are symmetry restricted. Modulating functions are: $u_i(t) = \sum_{n=1,2} A_{n,i}\cos[2\pi(nt + \varphi_{n,i})]$, $i = x,y,z$. Standard deviations are given in parentheses.

	x	y	z	U (or U_{eq})
S	0.2500	0.1380 (1)	0.0000	0.015 (1)
Cl	0.03032 (2)	0.9377 (1)	0.15944 (3)	0.028 (1)
O	0.22528 (4)	−0.0080 (2)	−0.0951 (1)	0.020 (1)
C(1)	0.18652 (4)	0.3583 (2)	0.0448 (1)	0.015 (1)
C(2)	0.1345 (1)	0.4210 (2)	−0.0269 (1)	0.019 (1)
C(3)	0.0861 (1)	0.6010 (3)	0.0079 (1)	0.021 (1)
C(4)	0.0902 (1)	0.7107 (2)	0.1143 (1)	0.020 (1)
C(5)	0.1414 (1)	0.6460 (2)	0.1861 (1)	0.020 (1)
C(6)	0.1901 (1)	0.4686 (2)	0.1509 (1)	0.018 (1)
H(2)	0.1330 (8)	0.338 (4)	−0.099 (1)	0.011 (1)
H(3)	0.0484 (8)	0.651 (3)	−0.036 (1)	0.011 (1)
H(5)	0.1419 (8)	0.711 (4)	0.257 (1)	0.011 (1)
H(6)	0.2273 (8)	0.421 (3)	0.201 (1)	0.011 (1)

	$A_{n,x}$	$\varphi_{n,x}$	$A_{n,y}$	$\varphi_{n,y}$	$A_{n,z}$	$\varphi_{n,z}$
S	−0.00453 (2)	0.388 (1)	0.0000*	0.000*	0.02053 (4)	0.3190 (3)
	0.0000*	0.0000*	0.0015 (3)	0.23 (3)	0.0000*	0.0000*
Cl	0.01112 (2)	−0.0583 (3)	0.0582 (1)	−0.1424 (3)	0.01571 (4)	−0.1787 (4)
	−0.0036 (4)	0.00 (2)	−0.011 (1)	−0.06 (2)	−0.0029 (7)	−0.07 (4)
O	−0.0065 (1)	−0.438 (1)	−0.0145 (2)	0.226 (2)	0.0220 (1)	−0.580 (1)
	−0.0007 (1)	−0.04 (2)	−0.0025 (5)	−0.004 (3)	0.0004 (2)	0.01 (8)
C(1)	−0.0042 (1)	0.067 (2)	0.0169 (3)	0.355 (3)	0.0188 (1)	0.170 (1)
	−0.0003 (1)	−0.04 (9)	0.0008 (7)	0.8 (1)	−0.0008 (2)	−0.17 (4)
C(2)	−0.0030 (1)	−0.083 (4)	−0.0370 (3)	0.785 (1)	0.0163 (1)	0.138 (1)
	−0.0006 (2)	−0.04 (4)	−0.0039 (6)	−0.07 (3)	0.0018 (3)	−0.75 (2)
C(3)	−0.0057 (1)	−0.282 (2)	0.0498 (3)	0.137 (1)	0.0152 (1)	0.030 (1)
	0.0010 (2)	0.00 (2)	0.0069 (6)	0.06 (2)	0.0020 (3)	−0.08 (2)
C(4)	0.0078 (1)	0.155 (1)	0.0415 (3)	0.048 (1)	0.0166 (1)	−0.048 (1)
	0.0019 (1)	−0.14 (1)	0.0065 (6)	−0.13 (2)	0.0023 (3)	−0.21 (2)
C(5)	−0.0080 (1)	−0.244 (1)	0.0210 (3)	0.120 (2)	0.0187 (1)	−0.021 (1)
	0.0015 (2)	−0.02 (2)	0.0046 (7)	−0.12 (3)	0.0017 (2)	−0.06 (2)
C(6)	−0.0066 (1)	−0.051 (2)	−0.0097 (3)	−0.182 (5)	0.0200 (1)	0.091 (1)
	0.0009 (2)	0.15 (3)	−0.0009 (7)	−0.4 (1)	−0.0010 (2)	0.75 (4)
H(2)	−0.0010 (9)	−0.0 (1)	−0.042 (4)	0.85 (2)	0.019 (2)	0.20 (1)
H(3)	−0.0071 (9)	−0.37 (2)	0.077 (5)	0.10 (1)	0.017 (2)	−0.01 (2)
H(5)	−0.0120 (9)	−0.28 (1)	0.022 (4)	0.15 (3)	0.025 (2)	−0.10 (1)
H(6)	−0.0091 (9)	0.04 (2)	−0.013 (4)	0.13 (5)	0.024 (2)	0.13 (1)

* Lists of structure factors and anisotropic thermal parameters have been deposited with the British Library Document Supply Centre as Supplementary Publication No. SUP 71316 (33 pp.). Copies may be obtained through The Technical Editor, International Union of Crystallography, 5 Abbey Square, Chester CH1 2HU, England. [CIF reference: AL0558]

Table 4. *Interatomic distances* (Å) *in the incommensurate phase of DCBPS*

d_{min}, d_{max} and d_{av} and the minimum, maximum and average values of the modulated distances, respectively. Δ is the difference between the extremal distances. E.s.d.'s are given in parentheses.

	d_{min}	d_{max}	Δ	d_{av}
S—O	1.438 (2)	1.446 (2)	0.009	1.443 (2)
S—C(1)	1.762 (1)	1.766 (3)	0.003	1.764 (3)
Cl—C(4)	1.717 (3)	1.755 (3)	0.038	1.735 (3)
C(1)—C(2)	1.389 (4)	1.403 (4)	0.014	1.397 (4)
C(2)—C(3)	1.369 (4)	1.403 (4)	0.034	1.386 (4)
C(3)—C(4)	1.388 (4)	1.405 (4)	0.017	1.395 (4)
C(4)—C(5)	1.374 (4)	1.403 (4)	0.030	1.387 (4)
C(5)—C(6)	1.367 (4)	1.398 (4)	0.031	1.383 (4)
C(1)—C(6)	1.385 (3)	1.400 (3)	0.015	1.392 (3)
C(2)—H(2)	0.922 (19)	1.022 (18)	0.100	0.958 (19)
C(3)—H(3)	0.932 (18)	1.005 (18)	0.073	0.968 (18)
C(5)—H(5)	0.831 (19)	0.991 (19)	0.159	0.916 (19)
C(6)—H(6)	0.973 (18)	1.019 (18)	0.046	0.993 (18)

Table 5. *Bond angles* (°) *in the incommensurate phase of DCBPS*

	a_{min}	a_{max}	Δ	a_{av}
C(2)—C(1)—C(6)	120.9 (4)	122.3 (4)	1.34	121.6 (4)
C(1)—C(2)—C(3)	118.4 (4)	119.8 (4)	1.45	119.1 (4)
C(2)—C(3)—C(4)	117.8 (4)	120.1 (4)	2.26	118.9 (4)
C(3)—C(4)—C(5)	121.1 (4)	123.2 (4)	2.10	122.1 (4)
C(4)—C(5)—C(6)	118.8 (4)	119.5 (4)	0.77	119.1 (4)
C(5)—C(6)—C(1)	118.7 (4)	119.8 (4)	1.05	119.3 (4)
O—S—C(1)	107.1 (2)	107.4 (2)	0.26	107.3 (2)
C(3)—C(4)—Cl	119.2 (3)	120.1 (3)	0.96	119.6 (3)

4. Discussion

A single DCBPS molecule and a projection along the *b* axis showing the packing in the average structure are shown in Fig. 1. Apart from the thermal parameters, the average structure does not show any significant differences from the room-temperature structure (Sime & Woodhouse, 1974). The phenyl groups retain their planarity. The largest differences appear in the relative orientation of the phenyl groups, described by the dihedral angle, Φ_T, between the plane of the aromatic ring and the plane defined (see Fig. 1*a*) by the least-squares axes S—C(1)—C(4)—Cl and S—C(1)′—C(4)′—Cl′ [Cl′, C(4)′ and C(1)′ are related to Cl, C(4) and C(1) by the twofold axis of the molecule]. Also, the 'bending' angle of the molecule, Φ_B, between these two latter axes shows a significant change. In the average structure these angles are $\Phi_T = 83$ and $\Phi_B = 101.7°$, while at room temperature the values are $\Phi_T = 84.6$ and $\Phi_B = 104.6°$.

The modulation amplitudes of the non-H atoms are about 0.1 Å with the largest values 0.29 Å along the *y* direction for the Cl atom and 0.27 Å along the *z* direction for the O atom. For the H atoms, the refined modulation parameters indicate that the modulations of these atoms are in phase with those of the C atoms to which they are bonded. However, this result and the modulation amplitudes must be treated with caution as the contribution of these atoms to the diffraction pattern is very small.

The contribution of the second harmonic to the atomic modulation depends on the atom, being larger for the Cl atom and smaller for the C(1) atom; plots of the modulation of both atoms are given in Fig. 2. The plotted functions are:

$$u_i(\mu,v) = a_{1,i}(\mu)\cos\{2\pi[\mathbf{q}.\mathbf{r}_0(\mu) + \varphi_{1,i}(\mu) + v]\} + a_{2,i}(\mu)\cos\{2\pi[2\mathbf{q}.\mathbf{r}_0(\mu) + \varphi_{2,i}(\mu) + 2v]\} \quad (5)$$

where v is the continuous variable $\mathbf{q}.\mathbf{l}$, $i = x, y, z$ and $a_{n,i}(\mu)$, $\varphi_{n,i}(\mu)$ and $\mathbf{r}_0(\mu)$ are the refined amplitudes, phases and average positions given in Table 3. The continuous variable $v = \mathbf{q}.\mathbf{l}$ (mod. 1) takes all values from 0 to 1 when $\mathbf{l}$ runs over all cells in the crystal and so the functions represented in Fig. 2 give all the possible atomic displacements in the crystal resulting from the modulation. Similarly, the modulated functions of the interatomic distances and bond angles can be obtained by calculating these magnitudes for

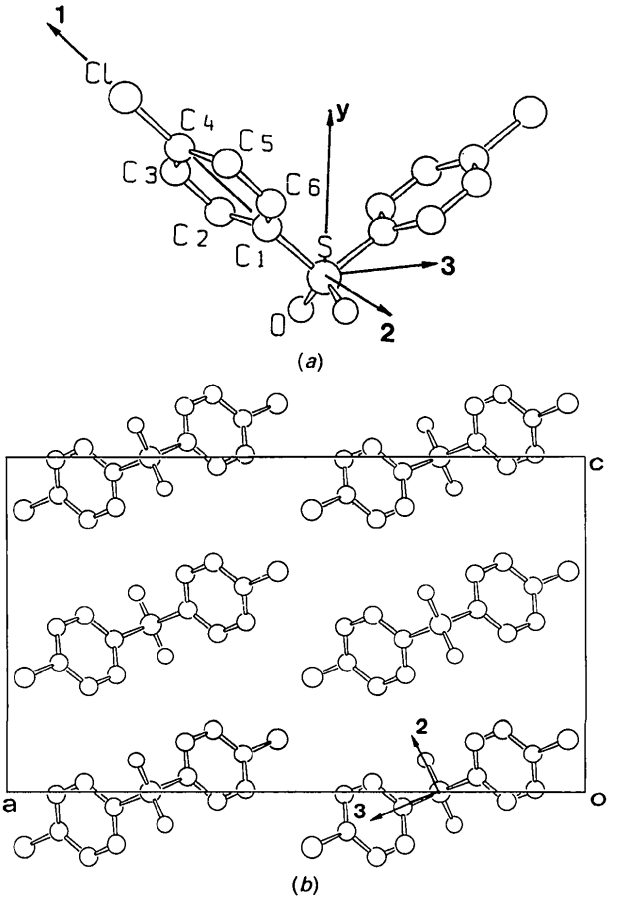

Fig. 1. (*a*) Scheme of the DCBPS ($C_{12}H_8Cl_2O_2S$) molecule (H atoms excluded). (*b*) *ac* projection of the average structure at 90 K. Axes labelled 1, 2 and 3 are used in the description of the structural modulation in terms of rotations and translations of the chlorophenyl groups in §4.

different values of v, that is, in different cells; the results are summarized in Tables 4 and 5.

Similar plots for all the C atoms to those given in Fig. 2 show clearly that their modulations for each direction are approximately in phase. In addition, from Tables 4 and 5, it can be seen that variations of interatomic distances and intramolecular angles of the chlorophenyl group in the incommensurate structure are very small. It can also be shown that the aromatic ring retains its planarity in the modulation. This suggests that the atoms within the chlorophenyl groups behave as approximately rigid units. If this is the case, then the structural modulation can be interpreted in terms of rigid-body motions (rotations plus translations) of the DCBPS molecule as a whole, and additional intramolecular twists and relative rotations of the two chlorophenyl groups so as to keep the bonded structure of the whole molecule essentially undistorted. The intramolecular distortion can be described by variations along the modulation of the angles Φ_T and Φ_B, defined above. Both angles have been calculated for different values of the coordinate $v = \mathbf{q}.\mathbf{l}$, using the atomic coordinates given by (1) and (2) and the parameters of Table 3. The results, which are plotted in Fig. 3, show that the structural modulation involves an anharmonic modulation of the dihedral angle Φ_T of the molecule with a maximum amplitude of 3.3° and, a double harmonic modulation of the bending angle Φ_B with an amplitude of 1.5°.

A full description of the structural modulation within a rigid-body approximation for the chlorophenyl groups was carried out by means of the following fitting process: for a set of basic cells consecutive along the b axis, the individual atomic displacements of the S, C and Cl atoms in the asymmetric unit were fitted to a rigid-body motion consisting of three rotations plus three translations of the average configuration, around and parallel to the crystallographic axis, respectively. The centre of the rotations was fixed on the centre of mass of the average configuration of the whole DCBPS molecule and the rotations were treated according to the small-angle approximation. Agreement between the observed individual atomic displacements and the hypothetical rigid-body motions was expressed by the index $D = (\sum|d_{cal} - d_{obs}|^2/\sum|d_{obs}|^2)^{1/2}$ where d_{obs} and d_{cal} are the observed and calculated atomic displacements, respectively, relative to the average configuration of the molecular group. The D value obtained from the fitting at each consecutive cell is always rather small; it ranges between 3 and 12%,

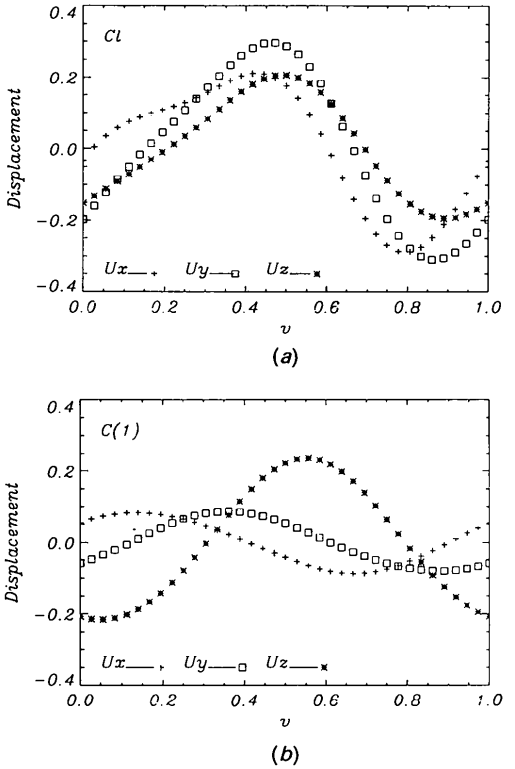

Fig. 2. Atomic modulation functions of the atoms Cl (a) and C(1) (b). The displacements are given in Å.

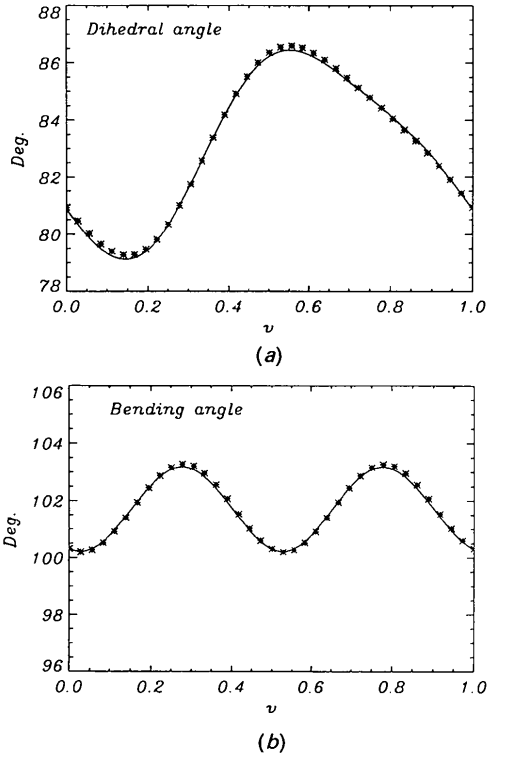

Fig. 3. Plot of the modulation of the dihedral and bending angles, Φ_T (a) and Φ_B (b), of the DCBPS molecule. Experimental values are represented by asterisks and the solid curve shows the results obtained from the rigid-body fitting shown in Table 6(b). Definitions of angles are given in the text.

the larger values being associated with those cells having smaller atomic displacements. This result confirms that the assumption of essentially rigid chlorophenyl groups is correct.

The fitted rigid-body motions of the asymmetric sulfur + chlorophenyl group, obtained for each consecutive cell can be considered along the continuous variable $v = \mathbf{q}.\mathbf{l}$ (mod. 1) as individual points of the associated rotational and translational modulation functions. Hence, these values can be fitted to the functions:

$$R_\alpha = R^1_\alpha \cos[2\pi(\mathbf{q}.\mathbf{r}_0 + v + \varphi^1_\alpha)] + R^2_\alpha \cos[2\pi(2\mathbf{q}.\mathbf{r}_0 + 2v + \varphi^2_\alpha)]$$
$$T_\alpha = T^1_\alpha \cos[2\pi(\mathbf{q}.\mathbf{r}_0 + v + \eta^1_\alpha)] + T^2_\alpha \cos[2\pi(2\mathbf{q}.\mathbf{r}_0 + 2v + \eta^2_\alpha)] \quad (6)$$

with $\alpha = x, y, z$, and $\mathbf{r}_0$ being the centre of mass of the complete (average) DCBPS molecule. (R^n_α/T^n_α) and $(\varphi^n_\alpha/\eta^n_\alpha)$, $n = 1, 2$, are then the first- and second-harmonic amplitudes and phases, respectively, of the rotational and translational modulation functions that describe the motion of the symmetry-independent chlorophenyl group. The results of the fitting process are summarized in Table 6(*a*) and Fig. 4.

As the first harmonic of the sulfur displacement along the *b* axis is forced to be zero by the superspace symmetry [see (4)], a non-zero amplitude of the modulation T_y in the fitting process would imply deformation of the bonded structure of the molecule. The value obtained for the amplitude of T_y is indeed very small (see Table 6*a*) and confirms the validity of the present semi-rigid model of the DCBPS molecule; its value of 0.02 Å can be considered an estimation of the magnitude of the error and noise in the fitting process.

A more physical picture of structural distortion in the modulated phase can be obtained if the global rotation–translation, given by the modulation functions $R_x(v)$, $R_y(v)$ and $R_z(v)$, $T_x(v)$ and $T_z(v)$, is described in terms of its components along the natural axes of the molecule indicated in Fig. 1(*a*). These are labelled in the following way: 1 for the line through atoms S—C(1)—C(4)—Cl, 2 for the axis perpendicular to the C(1)—S—C′(1) plane, 3 for the line perpendicular to 2 and the *y* axis (see Fig. 1).

Transformation of the rotational–translational modulation to the new axes is summarized in Table 6(*b*). Rotational modulation around axis 1 corresponds to modulation of the dihedral angle Φ_T, already calculated by other means and plotted in Fig. 3(*a*). In this same figure, the modulation as given by the results of Table 6(*b*) is also plotted in order to show the agreement between the two methods.

The structural modulation can be further analyzed in terms of frozen phonon modes. From the detected

Table 6. *Amplitudes and phases of the rotational and translational modulation functions of the* C_6ClS *group describing the structural modulation in DCBPS, for two different reference systems*

In (*a*) subscripts $a = x, y, z$ refer to crystallographic axes. Second harmonics for T_x and T_z are negligible. In (*b*) the components refer to the axes defined in the text and shown in Fig. 1. The values given in (*b*) represent the complex amplitudes of the nine symmetry modes described in Fig. 5, observed in the incommensurate structure of DCBPS. Rotations are given in °, translations in Å and phases in 2π units.

	R^1_α/T^1_α	$\varphi^1_\alpha/\eta^1_\alpha$	R^2_α/T^2_α	$\varphi^2_\alpha/\eta^2_\alpha$
(*a*)				
R_x	1.6	0.19	0.4	0.40
R_y	2.2	0.48	0.6	0.99
R_z	4.3	0.68	0.8	0.65
T_x	0.09	0.30	–	–
T_y	0.02	0.44	0.01	0.62
T_z	0.28	0.05	–	–
(*b*)				
R_1	3.5	0.48	0.6	0.78
R_2	3.3	0.68	0.7	0.62
R_3	3.5	0.32	–	–
R_y	–	–	0.7	0.10
T_3	0.14	0.95	–	–
T_2	0.26	0.07	–	–
T_y	–	–	0.01	0.62

extinction rule, or the corresponding superspace group, the symmetry of the order parameter of the phase transition can be identified (Pérez-Mato, Madariaga & Tello, 1984) as the irreducible representation Λ_2 (antisymmetric for C_{2v}) of the space group $I2/a$, along the line Λ of the Brillouin zone

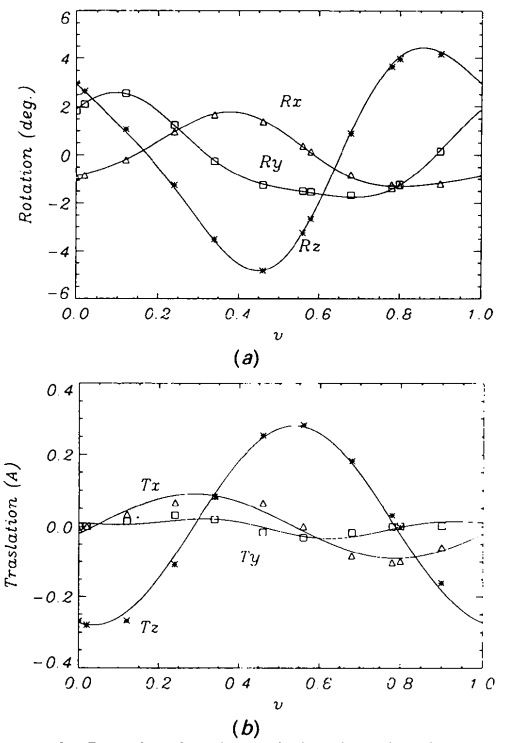

Fig. 4. (*a*), (*b*). Rotational and translational modulations resulting from fitting of the individual atomic displacements of the chlorophenyl group plus S atom to rigid-body motions.

(Bradley & Cracknell, 1972). Indeed, the symmetry restrictions given by (3) between symmetry-related modulation functions, imply that the first harmonic of the modulation corresponds to a frozen Λ_2 mode, while the second harmonic is a frozen mode of Λ_1 symmetry. From (3), the structure of the possible symmetry modes participating in a mode of Λ_2 or Λ_1 symmetry can be anticipated. A scheme of their polarization vectors is shown in Figs. 5(*a*) and 5(*b*). The calculated amplitudes and phases listed in Table 6(*b*) represent, in fact, the complex amplitudes of these five Λ_2 and four Λ_1 symmetry modes, present in the first and second harmonic, respectively, of the observed modulation. It can be seen in Fig. 5(*b*) that the second-harmonic $R_2(\Lambda_1)$ rotation represents one half of the variation of the bending angle Φ_B (no other mode distorts this angle). This explains the wavelength of the Φ_B modulation observed in Fig. 3(*b*). Indeed, the second-harmonic $R_2(\Lambda_1)$ rotation doubled in amplitude, over the average value of Φ_B, has been also drawn in Fig. 3(*b*), showing the coincidence between the two independent determinations.

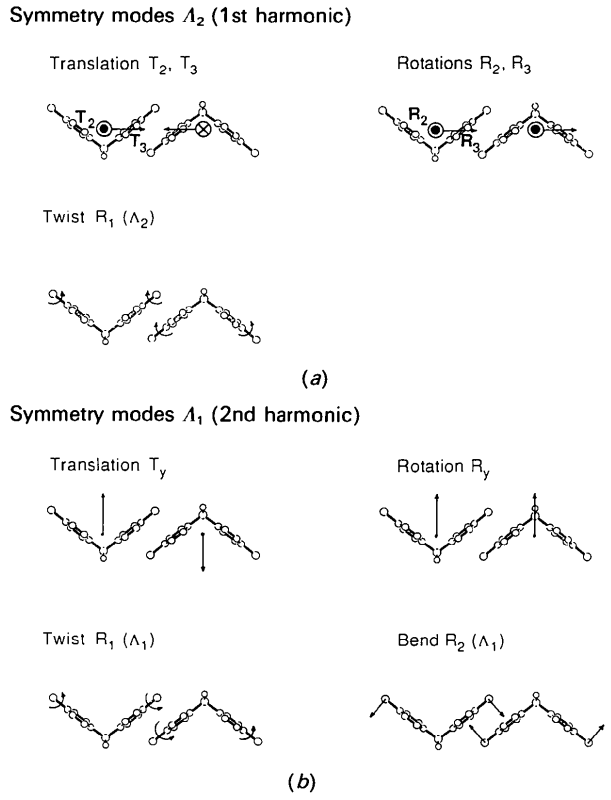

Fig. 5. Scheme of the allowed Λ_2 (*a*) and Λ_1 (*b*) symmetry modes for the basic structure of DCBPS, within a rigid approximation of the chlorophenyl groups, whose amplitudes in the actual incommensurate structure of DCBPS are given in Table 6(*b*). The motion of the two molecules in the primitive unit cell are represented in a projection along the axis labelled 2 in Fig. 1. The figure indicates the relation between the amplitudes (A and B) of the motions in one molecule and its inversion-related one, when these are represented in the form $A\cos\{2\pi[\mathbf{q}.(\mathbf{l}+\mathbf{r}_0^1)+\varphi]\}$ and $B\cos\{2\pi[\mathbf{q}.(\mathbf{l}+\mathbf{r}_0^2)-\varphi]\}$, respectively, where $\mathbf{r}_0^1$ and $\mathbf{r}_0^2$ are the centres of mass of the two molecules. Therefore, the actual phase shift between the motions of the two molecules is not in general 0 or π, but depends on the value of the phase φ in one of them as given in Table 6(*b*).

In the first harmonic, only the mode $R_1(\Lambda_2)$ (see Fig. 5*a*) distorts the DCBPS molecule and represents an internal molecular degree of freedom, while in the second harmonic, in addition to the $R_2(\Lambda_1)$ mode, already mentioned above, a second $R_1(\Lambda_1)$ causes a molecular distortion and is the origin of the anharmonicity of the Φ_T modulation observed in Fig. 3(*a*). It is important to note that the $R_1(\Lambda_2)$ mode is the only one that breaks the local twofold symmetry of the molecules and the combination of modes $R_1(\Lambda_2)$ and $R_1(\Lambda_1)$ means that in general the magnitudes of the twisting angles of the two chlorophenyl groups in the same molecule are different.

In summary, the results of Table 6(*b*) indicate that the structure of the order-parameter distortion is quite complex. Although it can be viewed to a good approximation as a distortion which keeps the bonded distances unchanged, it involves, with similar weights, all symmetry-allowed degrees of freedom within a semi-rigid representation of the molecule. The only intramolecular distortion participating in the order parameter represents a π out-of-phase twist of both chlorophenyl groups around their corresponding S—Cl axes. The angle C(1)—S—C(1′) only varies in the modulation as a consequence of a secondary distortion of different symmetry than that of the order parameter.

The lattice-dynamics calculations reported by Saito, Kikuchi & Ikemoto (1992) for a simple force model seem to be in accordance with the present structural analysis. Although not indicated explicitly, the soft-phonon branch observed in the model seems to have Λ_2 symmetry, consistent with the previous order-parameter identification. The eigenvector of the soft-mode is reported to have, apart from the $R_1(\Lambda_2)$ twist mode, a significant translational and rotational component of the whole molecule, as observed in the frozen modulation.

Although experimentally no lock-in phase transition seems to occur as temperature is decreased, it may be of interest to predict the possible symmetry of the commensurate structure resulting from an eventual lock-in of the modulation wavevector at $\mathbf{q} = \mathbf{b}^*$. A simple analysis of the irreducible representation Λ_2 reduced at the point $\mathbf{q} = \mathbf{b}^*$ yields as possible space groups for the virtual lock-in phase: $P2_1/a$, $P2_1/c$ or $P2_1$ depending on the direction taken by the order parameter. According to this analysis it is possible that a strong electric field applied along the monoclinic axis could be enough to stabilize a polar $P2_1$ phase at $\mathbf{q} = \mathbf{b}^*$.

The authors thank Dr Pusiol for his private communication pointing out the interest in this compound and its probable incommensurate phase, before any diffraction confirmation existed. We also gratefully acknowledge the help of Dr J. Fabry in the precession camera experiments. This work was supported by the Spanish DGICYT project No. PB91-0448.

References

BRADLEY, C. J. & CRACKNELL, A. P. (1972). *The Mathematical Theory of Symmetry in Solids*. Oxford: Clarendon Press.

CAILLEAU, H. (1986). *Incommensurate Phases in Dielectrics*, Vol. 2, ch. 12, edited by R. BLINC & A. P. LEVANYUK. *Modern Problems in Condensed Matter Sciences*. Amsterdam: North Holland.

COSIER, J. & GLAZER, A. M. (1986). *J. Appl. Cryst.* **19**, 105–107.

ETRILLARD, J., EVEN, J., SOUGOTI, M., LAUNOIS, P., LONGEVILLE, S. & TOUDIC, B. (1993). In preparation.

ETRILLARD, J., TOUDIC, B., BERTAULT, M., EVEN, J., GOURDJI, M., PÉNEAU, A. & GUIBÉ, L. (1993). In preparation.

ISHII, K., NAKAYAMA, H., SAKATO, T. & KANO, H. (1992). *J. Phys. Soc. Jpn*, **61**(7), 2317–2326.

JANNER, A. & JANSSEN, T. (1980). *Acta Cryst.* A**36**, 399–415.

KASANO, H., KOSHIBA, T., KASATANI, H. & TERAUCHI, H. (1990). *J. Phys. Soc. Jpn*, **39**(2), 408–411.

NAKAYAMA, H., EGUCHI, T. & KISHITA, M. (1992). Proc. XIth Int. Symp. Nucl. Quadrupole Reson. Spectrosc., London, Abstracts, pp. 232–248.

PACIOREK, W. A. & KUCHARCZYK, D. (1985). *Acta Cryst.* A**41**, 462–466.

PACIOREK, W. A. & USZYNSKI, I. (1987). *J. Appl. Cryst.* **20**, 57–59.

PÉREZ-MATO, J. M., MADARIAGA, G. & TELLO, M. J. (1984). *Phys. Rev. B*, **30**, 1534–1543.

PÉREZ-MATO, J. M., MADARIAGA, G., ZÚÑIGA, F. J. & GARCIA-ARRIBAS, A. (1987). *Acta Cryst.* A**43**, 216–226.

PUSIOL, D. J., WOLFENSON, A. E. & BRUNETTI, A. H. (1989). *Phys. Rev. B*, **40**(1), 2523–2528.

SAITO, K., KAMIO, H., KIKUCHI, K. & IKEMOTO, I. (1990). *Thermochim. Acta*, **163**, 241–248.

SAITO, K., KIKUCHI, K. & IKEMOTO, I. (1992). *Solid State Commun.* **81**(3), 241–243.

SIME, J. G. & WOODHOUSE, D. I. (1974). *J. Cryst. Mol. Struct.* **4**, 287–303.

STEWART, J. M., KRUGER, G. J., AMMON, H. L., DICKINSON, C. W. & HALL, S. R. (1972). *The XRAY72 System*. Version of June 1972. Technical Report TR-192. Computer Science Centre, Univ. of Maryland, College Park, Maryland, USA.

TANAKA, T., SAITO, K., NAKAYAMA, H., EGUCHI, T. & ATAKE, T. (1991). 61st Autumn Meet. Chem. Soc. Jpn. Abstract 2B108.

WOLF, P. M. DE, JANSSEN, T. & JANNER, A. (1981). *Acta Cryst.* A**37**, 625–636.